

Proceedings of the International Conference on Oxide Materials for Electronic Engineering, May 29–June 2, 2017, Lviv

Structure and Catalytic Properties of Co–Fe Systems in the Reaction of CO₂ Methanation

M. ZHLUDENKO^a, A. DYACHENKO^a, O. BIEDA^{a,*}, S. GAIDAI^a, M. FILONENKO^b
AND O. ISCHENKO^a

^aTaras Shevchenko National University of Kyiv, 64/13 Volodymyrs'ka Str, Kyiv, 01601, Ukraine

^bNational Pedagogical Dragomanov University, 9 Pirogova Str., Kyiv, 01601, Ukraine

The properties of Fe–Co catalysts in the reaction of CO₂ hydrogenation were investigated. Samples with high cobalt concentrations have shown higher activity. Morphology of the obtained catalysts was observed by using scanning electron microscopy and the elemental composition of surface of the catalysts was determined by scanning electron microscopy-energy dispersive X-ray method. Energy dispersive X-ray analysis showed that metal distribution is not homogeneous with various metal ratio in selected points of the surface for the Fe-rich less active samples, whereas for the Co-rich samples with higher activity metals are homogeneously distributed, which is possibly connected to the formation of single phase.

DOI: [10.12693/APhysPolA.133.1084](https://doi.org/10.12693/APhysPolA.133.1084)

PACS/topics: 82.30.Hk, 82.30.-b, 82.20.-w

1. Introduction

State of the environment and the greenhouse problem are still ones of the most pronounced ecological problems. The increase in CO₂ emissions leads, in particular, to the negative climatic changes.

The CO₂ hydrogenation process (the Sabatier reaction) is one of the effective methods of removal of CO₂, allowing not only to utilize its excess but to convert it into light hydrocarbons, opening the way to the new sources of fuel [1, 2].

One of the most perspective ways to solve the mentioned tasks is so-called power-to-gas technology. The concept is to use the excess of energy to split water into H₂ and O₂, with further conversion of hydrogen and carbon dioxide into methane. Thus, the renewable energy can be stored in the already existing network of the natural gas, utilizing its great volumes. Moreover, natural gas is a convenient fuel that is already widely used in different aspects of human life, and does not show the security problems connected with use of gaseous hydrogen [3, 4].

CO₂ hydrogenation depending on the conditions and the type of catalyst used gives a wide spectrum of products, from CO and CH₄ to ethylene and higher hydrocarbons. Literature data are present on studies of metallic catalysts based on transition metals (Ni, Co, Fe, Mn, Cu, Zn etc.) [5–8] as well as on the noble ones (Pt, Pd, Ru, Rh etc.) [9, 10]. From the economical point of view, use of non-noble metals is more proficient [11, 12].

No common point of view on the mechanism of the Sabatier reaction exists at the time. The significant part of potential combinations of active phase, promoter and

support remains not examined yet. It is desired to create thermally and mechanically stable catalysts that possess highly specific surface. Thus, it can be stated that the search of cheap catalysts compliant with the above-mentioned is an actual task.

2. Experimental

A series of metallic samples based on Fe and Co with different Co:Fe ratio was obtained as below. The calculated amounts of metals were dissolved in the concentrated nitric acid, the solution was cooled to room temperature (r.t.) and hydroxides were precipitated by excess of NH₃ solution. The precipitate after the evaporation was dried at 180 °C and pre-reduced in flow of 50% H₂ in helium for 2 h at 350 °C.

The catalytic activity of the samples was studied in a fixed bed reactor in flow of 2% CO₂+ 55% H₂ mixture (balanced with He), at total flow of 100 cm³/min and sample mass of 1 g. The reactor with inner diameter of 8 mm contained a 1 mm glass tube with a thermocouple inside, put in the catalyst bed. The pre-treatment of sample in the reaction mixture was made by gradual increase of the catalyst temperature to 450 °C over 3 h. The exiting gaseous mixture was analyzed by gas chromatograph with a thermal conductivity detector (Shimadzu GC-2014, 1 m length packed column, molecular sieves 5A).

XRD studies of the samples were performed on a diffractometer MiniFlex 600 (Rigaku, Japan) with Co K_α radiation ($\lambda = 1.7903 \text{ \AA}$). The morphology of samples and the chemical analysis were studied on the TESCAN Mira 3 LMU scanning electron microscope (SEM) equipped with energy-dispersive X-ray (EDX) detector (Oxford INCA). The specific surface was assessed by adsorption of Ar at 77 K.

*corresponding author; e-mail: a_byeda@chem.knu.ua

3. Results and discussion

The dependence of catalytic activity on the composition of the sample is shown in Fig. 1. The temperature of 300 °C was taken for the ease of the comparison as at this temperature the most active sample (93% Co, 7% Fe) has reached 100% methane yield.

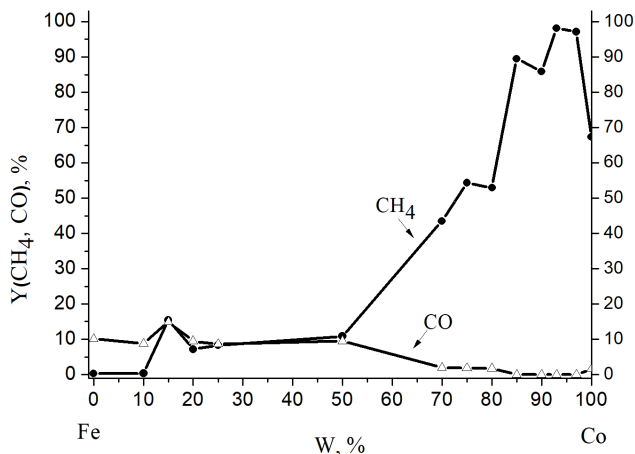


Fig. 1. Yield of reaction products at 300 °C versus composition of the catalyst.

The data signify that the most active samples are in the region of high Co content. The activity increases rapidly with Co content when it exceeds 50%. This can be explained by the fact that according to the phase diagram of Co-Fe system [13] an area of heterogeneity exists in this region of Co concentrations. A diffusionless transition from $\gamma + \alpha$ phases to ε phase occurs in the solid solutions, and the transition temperature decreases down to r.t. for 91–93% of Co (γ — face-centered cubic Co-Fe solution, α — normal body-centered cubic iron, ε — normal hexagonal Co). Hence, the most active samples are expected to contain γ phase only. It should be mentioned that CO, which is a byproduct, is present for the samples with high Fe content but completely absent for the samples with high Co content (>70%).

The characteristic catalytic curves (product yields versus temperature) are shown in Fig. 2 for the active (Co₉₃Fe₇) and the inactive (Co₁₄Fe₈₆) samples.

The active sample shows the start of reaction at 150 °C and the total conversion to methane at 300 °C, which is a remarkable result for this type of catalysts in comparison to literature data [14]. The total absence of CO co-product is noteworthy for this sample. For the inactive one, the reaction starts at around 200 °C, the highest methane yield achieved is only 48% at 350 °C and 10% of CO is present in the reaction mixture.

For the active catalyst (Fig. 3a,b) the more defective structure in comparison to the inactive one (Fig. 3c,d) is clearly seen in the micrometer-range magnification. In the nm range a close examination shows the agglomerates in the active sample (*ca.* 80–100 nm) and for the

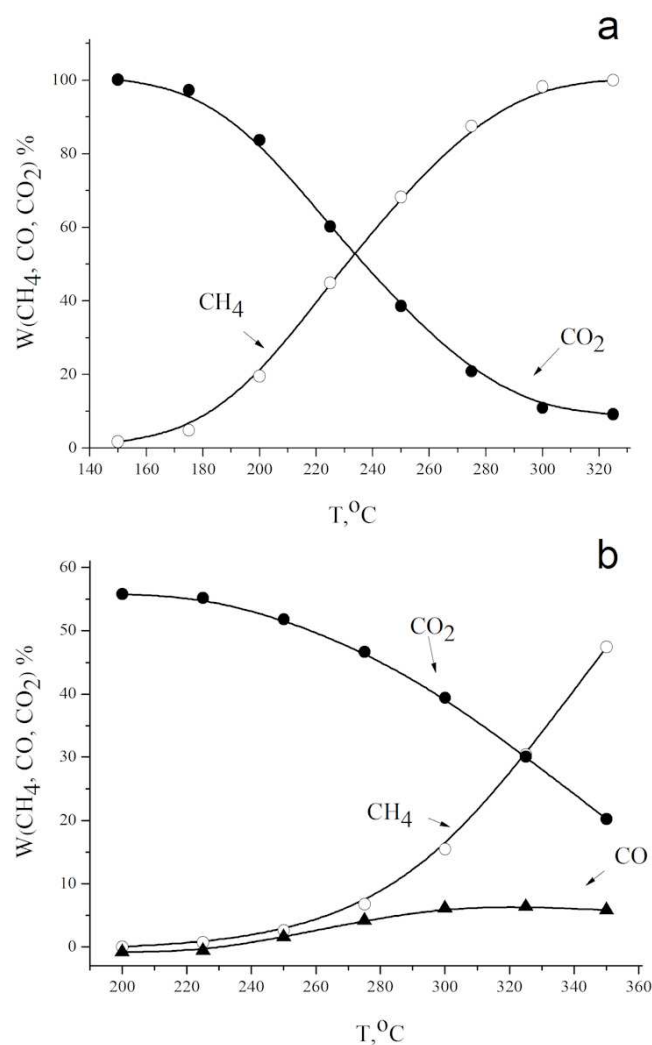


Fig. 2. Temperature dependences of CH₄ and CO yields for Co₉₃Fe₇ (a) and Co₁₄Fe₈₆ (b).

inactive one the big agglomerates presumably resulted from sintering are observed, but for Co₉₃Fe₇ the particle size is about 40 nm and for Co₁₄Fe₈₆ about 80 nm, the surface layer being much more defective for the former. The specific surface for all of the samples studied was about 18 m²/g, indicating no notable difference in the accessible surface.

The EDX data show that for the active sample the metal ratio found in different regions is effectively the same and equals to the one given by synthesis (Table I). Instead, a strictly uneven distribution of Co and Fe is revealed in the inactive one.

The macroscopic structure of the samples is also different. Co₉₃Fe₇ shows the several μm -sized aggregates with a porous surface, while Co₁₄Fe₈₆ shows the big aggregates in 10–50 μm range having the smooth surface. Size of the pores in the former is below 100 nm, indicating the presence of both micro- and mesopores. For

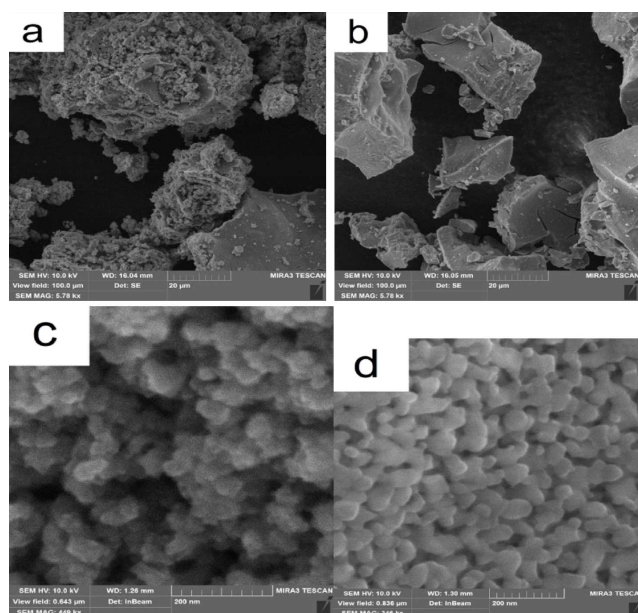


Fig. 3. Micrographs of $\text{Co}_{93}\text{Fe}_7$ sample ((a) 20 μm , (c) 200 nm) and $\text{Co}_{14}\text{Fe}_{86}$ sample ((b) 20 μm , (d) 200 nm).

SEM-EDX data for $\text{Co}_{93}\text{Fe}_7$ TABLE I

Region #	Content [at.%]			Fe:Co ratio	
	Fe	Co	O	by analysis	by synthesis
1	5.25	70.37	24.38	6.95:93.05	7:93
2	7.55	89.79	2.66	7.76:92.24	
3	9.20	84.40	6.40	9.83:90.17	
4	6.50	79.79	13.71	7.53:92.47	

$\text{Co}_{14}\text{Fe}_{86}$ one can mention a dense structure consisting of 70–80 nm spheroidal particles which are sintered in a thick layer. The elemental composition (see Table II) for this sample shows the inequality of metal ratios in different points to be of as high as 50%.

XRD analysis of $\text{Co}_{93}\text{Fe}_7$ before the reduction in the reaction mixture showed only a Co_3O_4 phase. However, after catalytic test the diffraction pattern of the reduced sample (Fig. 4a) shows both cubic and hexagonal (the latter with low intensity and broadening of the reflexes) metallic cobalt and CoO oxide phase, the oxide presumably being a result of exposition to air after the catalytic test.

SEM-EDX data for $\text{Co}_{14}\text{Fe}_{86}$ TABLE II

Region #	Content [at.%]			Fe:Co ratio	
	Fe	Co	O	by analysis	by synthesis
1	56.41	33.93	9.30	62.44:37.56	86:14
2	81.46	6.04	12.50	93.10:6.90	
3	69.00	11.06	19.94	86.19:13.81	
4	67.35	10.80	19.46	66.59:33.41	

Only iron oxides Fe_2O_3 and Fe_3O_4 are present in the pattern of the untreated, freshly synthesized $\text{Fe}_{86}\text{Co}_{14}$ sample. After the catalytic tests metallic $\alpha\text{-Fe}$ and the residual $(\text{Fe}, \text{Co})_3\text{O}_4$ are present (Fig. 4b).

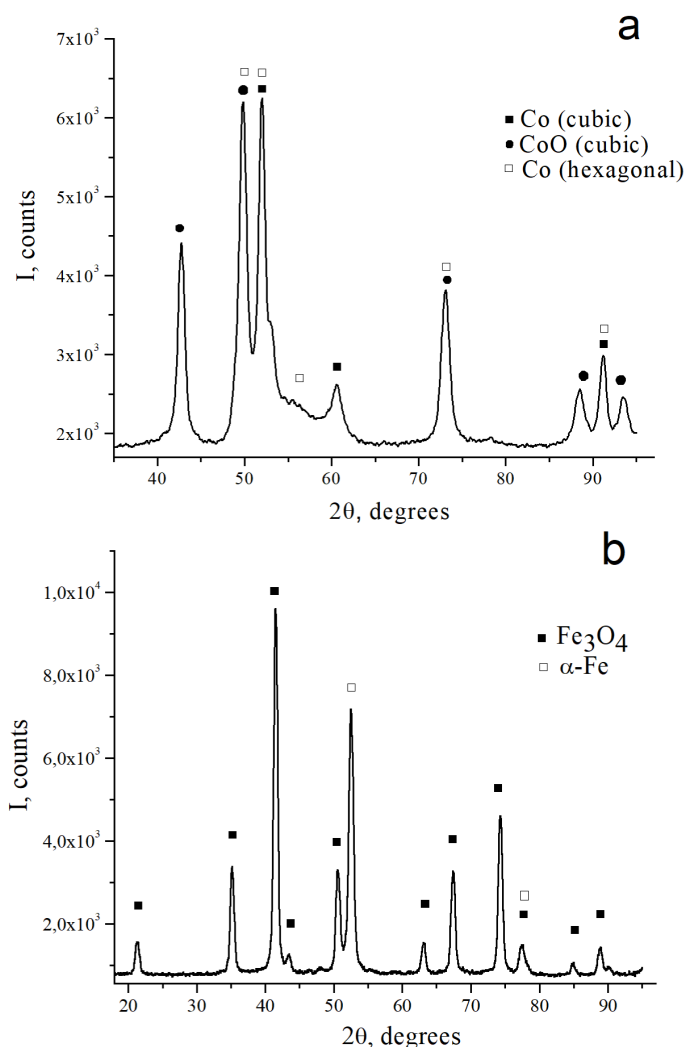


Fig. 4. XRD patterns of $\text{Co}_{93}\text{Fe}_7$ (a) and $\text{Co}_{14}\text{Fe}_{86}$ (b) samples.

4. Conclusions

A series of inexpensive Co–Fe catalysts of CO_2 hydrogenation was tested in the atmospheric pressure conditions. A sample with 7% Fe shows a pronounced catalytic activity and is primarily formed by cubic $\text{Co}(\text{Fe})$ phase, in agreement to Fe–Co phase diagram which shows one cubic alloy for this composition. This phase must be considered responsible for the high catalytic activity. Addition of small amount of Fe stabilizes the cubic phase and has an effect on morphology, promoting smaller particle size. Catalysts with high Fe content demonstrate poor activity instead.

References

- [1] J. Gao, Y. Wang, Y. Ping, D. Xu, G. Xu, F. Gu, F. Su, *RSC Adv.* **2**, 2358 (2012).
- [2] M. Jacquemin, A. Beuls, P. Ruiz, *Catal. Today* **157**, 462 (2010).
- [3] E. Giglio, A. Lanzini, M. Santarelli, P. Leone, *J. Energy Stor.* **1**, 22 (2015).
- [4] E. Giglio, A. Lanzini, M. Santarelli, P. Leone, *J. Energy Stor.* **2**, 64 (2015).
- [5] Bin Miao, Su Su Khine Ma, Xin Wang, Haibin Su, Siew Hwa Chan, *Catal. Sci. Technol.* **6**, 4048 (2016).
- [6] A. Westermann, B. Azambre, M. Bacariza, I. Graca, M. Ribeiro, J. Lopes, C. Henriques, *Appl. Catal. B* **59**, 314 (2015).
- [7] V. Budarin, V. Diyuk, L. Matzui, L. Vovchenko, T. Tsvetkova, M. Zakharenko, *J. Therm. Anal. Calorim.* **62**, 345 (2000).
- [8] Y.-G. Chen, K. Tomishige, K. Yokoyama, K. Fujimoto, *Appl. Catal. A Gen.* **165**, 335 (1997).
- [9] D.C. Upham, A.R. Derk, S. Sharma, H. Metiu, E.W. McFarland, *Catal. Sci. Technol.* **3**, 1783 (2015).
- [10] *Chemistry Handbook* Vol. 1, Ed. B.P. Nikolskiy, Chemistry, Moscow 1966) (in Russian).
- [11] J.J. Gamman, G.J. Millar, G. Rose, J. Drennan, *J. Chem. Soc. Faraday Trans.* **94**, 701 (1998).
- [12] W. Wang, S. Wang, X. Ma, J. Gong, *Chem. Soc. Rev.* **40**, 3369 (2011).
- [13] I. Ohnuma, H. Enoki, O. Ikeda, R. Kainuma, H. Ohtani, B. Sundman, K. Ishida, *Acta Mater.* **50**, 379 (2002).
- [14] W. Wang, Sh. Wang, X. Ma, J. Gong, *Chem. Soc. Rev.* **40**, 3703 (2011).